PROVENANCE DISCRIMINATION OF FRESHWATER PEARLS BY LA-ICP-MS AND LINEAR DISCRIMINANT ANALYSIS (LDA)

Artitaya Homkrajae, Ziyin Sun, Troy Blodgett, and Chunhui Zhou

This study investigates trace-element concentrations of 225 freshwater pearl samples using laser ablation–inductively coupled plasma–mass spectrometry (LA-ICP-MS) and subsequent statistical analysis using linear discriminant analysis (LDA). The samples consisted of three types: non-bead-cultured pearls (NBC) grown in China, natural pearls found in the United States, and cultured pearls (bead and non-bead) grown in the United States. By capturing variations in trace-element concentrations simultaneously through multivariate analysis, these supplementary techniques assist in identifying freshwater pearl origins with a greater degree of confidence.

With more than 300 native mussel species, the rivers and lakes of the United States have produced countless prized natural freshwater pearls over the centuries (Haag, 2012). America's rich freshwater pearling and shelling heritage has been recorded in the literature over the years. Natural pearls discovered in these waters have exhibited a wide range of shapes, colors, and surface characteristics (Kunz and Stevenson, 1908; Sweaney and Latendresse, 1984; Strack, 2006; Haag, 2012; Hsu et al., 2016). Overharvesting in the past by the shelling industry, dam construction, water pollution, siltation, and the introduction of non-native mussel species have damaged the habitat and shortened the lifespans of the indigenous mussels. Approximately 70% of the mussels are extinct, endangered, or of special concern (U.S. Fish & Wildlife Service, 2018). Wild mussels are still harvested under license in the states of Kentucky, Alabama, and Tennessee, and the shelling industry is heavily regulated (Watters et al., 2009; Hsu et al., 2016). Nevertheless, pearl production is currently very limited in the United States.

By contrast, the dominant source of freshwater cultured pearls—bead cultured and non-bead cultured (NBC)—is China, which developed NBC pearl cultivation during the 1990s in order to satisfy global demand for high-quality, affordable pearls. There are thousands of freshwater pearling farms in China; Zhuji, in Zhejiang Province, accounts for 85% of the total production (China Gems, 2019). The rest of the culturing operations are mainly situated in the southeastern part of China. *Hyriopsis* species mollusks are extensively used to culture Chinese freshwater pearls. The gemological characteristics of these pearls, as well as the culturing techniques applied, have been reported on previously (Scarratt et al., 2000; Akamatsu et al., 2001; Hua and Gu, 2002; Fiske and Shepherd, 2007). Freshwater NBC pearls are intentionally cultured without a solid shell bead nucleus, using just a piece of mantle tissue (epithelial cells) from donor mussels transplanted into a living host mussel. The grafted tissue later develops into a pearl sac and secretes calcium carbonate (nacre) as well as organic matter and water to form a pearl.

Real-time microradiography (RTX) and X-ray computed microtomography (μ-CT) are efficient techniques used by gemological laboratories to analyze a pearl's internal structure and determine whether it is natural or cultured (Karampelas et al., 2010, 2017; Krzemnicki et al., 2010). Most freshwater NBC pearls have distinct internal structures that can easily be identified by microradiography: twisted voids and elongated linear features in their center (Scarratt et al., 2000; Sturman, 2009). Nevertheless, some NBC pearls are challenging to accurately identify, as they contain small central growth features similar to those in some natural pearls. The identification can be further complicated if any drill holes are present or the pearls are mounted in jewelry, as these may cause the masking or removal of critical evidence.

See end of article for About the Authors and Acknowledgments.

GEMS & GEMOLOGY, Vol. 55, No. 1, pp. 47–60,
http://dx.doi.org/10.5741/GEMS.55.1.47

Figure 1. Representative freshwater pearl samples from the three sources studied: American natural pearls (top left), Chinese cultured pearls (center), and American cultured pearls (top right). Photo by Diego Sanchez.

Freshwater mussels are sedentary filter-feeders, and trace-element variability in such an organism can provide revealing information about their growth environment (Grabarkiewicz and Davis, 2008). The purpose of this study is to perform a preliminary investigation of the trace-element concentrations of natural pearls from North America and NBC pearls from China using laser ablation–inductively coupled plasma–mass spectrometry (LA-ICP-MS) and linear discriminant analysis (LDA) to separate these pearls by geographic origin, growth environment conditions, and mollusk species. LA-ICP-MS has become an important tool for gemstone identification due to its high spatial resolution, rapid and direct chemical analysis, and ultra-high sensitivity when measuring a wide range of elements (Abduriyim and Kitawaki, 2006). LDA is a type of multivariate analysis that can distinguish one class of object from another by applying weighted coefficients of multiple parameters—such as trace elements—to multiple functions representing each group such as USA-NAT, USA-CUL, and CH-NBC, potentially enhancing the benefits of the LA-ICP-MS analysis. This technique has already been applied to determine the country of origin of various gemstones (Blodgett and Shen, 2011; Pornwilard et al., 2011; Shen et al., 2013; Giuliani et al., 2014; Luo et al., 2015).

To augment the study, we also included a unique group of American freshwater cultured pearls. While not a major source for the pearl market, these serve as interesting samples since they were grown in very specific conditions in Kentucky Lake in the state of Tennessee. Washboard (*Megalonaias nervosa*) is a major mussel species used to culture American pearls. The culturing period takes three to five years, and the pearls were typically harvested in the autumn months of the year (Hsu et al., 2017). Thus their chemical compositions were expected to be more homogenous than those of the other sample bases.

MATERIALS AND METHODS

For LA-ICP-MS analysis, we selected 74 American natural (designated here as USA-NAT), 75 American cultured (USA-CUL), and 76 Chinese NBC freshwater pearls, all of various shapes, colors, and sizes (figure 1). Each loose pearl was analyzed in two or three spots (table 1). The variability of trace-element concentration in relation to the pearls' color was not considered in this study. All the American pearls were purchased from the American Pearl Company, Inc. (Nashville, Tennessee) and were claimed to be known samples from their collections (Hsu et al., 2017). These cultured pearls were reportedly grown in Kentucky Lake and harvested during different years. For the natural pearls reportedly collected from North American lakes and rivers, however, there is no exact record of the location, time, or mollusk species in which the pearls were formed. The Chinese pearls, mainly harvested from *Hyriopsis* mollusks, belong to the GIA research collection and were

TABLE 1. Freshwater pearls examined in this study.

Sample	Number	Weight range (ct)	Number of spots tested with LA-ICP-MS
American natural pearls (USA-NAT)	74	0.43–8.82	207
American cultured pearls (USA-CUL)			
• Non-bead cultured	61	0.26–4.35	168
• Bead cultured	14	2.43–8.16	42
Chinese non-bead-cultured pearls (CH-NBC)	76	1.39–5.65	213
Total	225		630

purchased from various sources over many years.

To confirm each pearl's identity before the chemical analysis, we examined their internal structures using RTX. The natural pearls showed a variety of structures that consisted mainly of concentric growth arcs following the pearl shape, with and without a dark organic spot in the center. Nine samples showed a questionable void structure that could be considered indicative of NBC pearl formation, though they resembled the other pearls in the group and most experienced pearl testers would consider their internal structures natural rather than NBC. The American NBC pearls revealed distinctive structures expected for this type of pearl. The majority exhibited relatively large void structures, some of which also contained small granular features. Some of the void features tended to be long and thin, appearing "linear" in form. The bead-cultured pearls showed bead nuclei with various shapes that related directly to their external appearance. The majority of the Chinese NBC samples had characteristic "twisted" void-like or elongated linear structures typical of freshwater NBC pearls. However, seven of them did not show any clear indication of a cultured origin because the evidence was entirely removed by the drilling process, leaving only the outer growth arcs, which are less diagnostic.

A MatriX-FocalSpot Verifier PF-100 X-ray fluorescence unit (100 kV and 3.2 mA excitation) equipped with a Canon EOS REBEL T4i DSLR camera (five-second exposure, F5.0, ISO 12800) was used to confirm the pearls' growth environment (either saltwater or freshwater) prior to advanced analysis. Most of the samples tested in the X-ray fluorescence unit showed moderate to strong greenish yellow fluorescence when exposed to X-rays due to the presence of trace amounts of manganese (Mn) (Hänni et al., 2005; Kessrapong et al., 2017), confirming their freshwater origin. Moreover, some freshwater pearls also exhibited an orangy reaction, which is probably related to Mn^{2+} in calcite composition and has been reported in freshwater pearls (Habermann et al., 2001; Dumańska-Słowik et al., 2008).

LA-ICP-MS. A Thermo Fisher Scientific iCAP Qc ICP-MS, coupled with a New Wave Research UP-213 laser ablation unit with a frequency-quintupled Nd:YAG laser (213 nm wavelength) running at 4 ns pulse width, was used for this study in GIA's Carlsbad laboratory. Ablation was achieved using a 55 μm diameter laser spot size, a fluence (energy density) of approximately 10–12 J/cm^2, and a 15 Hz repetition rate. ^{43}Ca was used as an internal standard, with a value of 400,400 ppmw calculated and rounded from pure calcium carbonate ($CaCO_3$). U.S. Geological Survey (USGS) pressed powder pellet carbonate standards (microanalytical reference materials MACS-1 and MACS-3) were used as matrix-matched external standards to minimize errors caused by matrix effects (Jochum et al., 2012). Argon was used as nebulizer gas (0.73 L/min), auxiliary gas (0.8 L/min), and cooling gas (14 L/min). Helium, used as part of the carrier gas, had a flow rate of 0.8 L/min. Argon and helium gas flow, torch position, sampling depth, and lens voltage were optimized for maximum sensitivity (counts per concentration) and low oxide production rates ($^{232}Th^{16}O/^{232}Th < 1\%$). Ablated material was then vaporized, atomized, and ionized by a plasma powered at 1550 W. Twenty-three different isotopes of interest were selected (table 2). When ablating a calcium carbonate matrix, interferences in the forms of molecules and ions with multiple charges produced by matrix compounds and a gas blank may produce inaccurate results (Jochum et al., 2012).

In Brief

- Pearl identification is still carried out primarily by observing and interpreting the internal structural results obtained from various X-ray techniques.
- Trace-element chemistry can be used to differentiate pearls formed in different environments.
- In the absence of definitive structural indicators, the combination of LA-ICP-MS and LDA can assist in identifying freshwater pearls with a greater degree of confidence.

BOX A: CHOOSING AN APPROPRIATE STATISTICAL MODEL FOR PREDICTING UNKNOWN SAMPLES

Selecting an appropriate prediction model may depend on many factors, such as the data type, the availability of training data, and the data distribution. For some data sets, no prior knowledge is available about the possible classes you wish to predict. When no training classes are available, cluster analysis which uses unsupervised learning can be applied (Hastie et al. 2008). Data can be continuous—as is the case for trace elements—or discrete, such as yes or no responses in a survey. Logistic regression is a good statistical tool for analyzing discrete data. For continuous data with known classes, there are a number of analytical tools available. LDA is a common statistical model and closely related to principle component analysis (PCA) and factor analysis. All look for linear combinations of variables that best explain the data (Martinez and Kak, 2001). LDA specifically models the differences between the classes while PCA does not; PCA is a better choice for distinguishing between classes when the class means are similar and there are large differences in variance. Quadratic discriminate analysis (QDA) can be used to draw nonlinear boundaries between classes, but like any other nonlinear fit, the data density needs to be high enough to prevent overtuning the model to a data scattering where no solid relationships really exist. QDA is only viable in situations where the ratio of the sample size to the variable count is large (Hastie et al., 2008). Logistic regression does not have as many assumptions and restrictions as discriminant analysis and therefore tends to be more universal. However, when discriminant analysis' assumptions are met, the LDA model tends to perform better than logistic regression (Hastie et al., 2008). Regularized discriminant analysis (RDA) is best for sample distributions that are strongly ellipsoidal (Friedman, 1989).

Table 2 shows major interferences of each isotope related to matrix and gas blank and indicates the minimum required mass resolving power (MRP) necessary for a particular mass being analyzed to make a separation from the corresponding interferences (table 2, column 6). The unit we used has two resolution modes: normal and high. Normal-resolution mode has a peak width of 0.7 atomic mass units (amu), which results in a 57 MRP at atomic mass 40 and a 429 MRP at atomic mass 300. High-resolution mode has a peak width of 0.3 amu, yielding a 133 MRP at atomic mass 40 and a 1000 MRP at atomic mass 300. If a required MRP for the separation of isotopes (table 2, column 6) is smaller than the MRP applied by LA-ICP-MS (table 2, column 7), the interferences related to the isotopes can be resolved. It is obvious that the MRP required for the separation of elements cannot be achieved with either resolution mode for almost all selected isotopes except ^{60}Ni. As a result, the analysis of isotopes with high interference signals (table 2, column 5) as discriminators must be carefully avoided. To optimize the signals, measurements were performed in high-resolution mode for ^{43}Ca and with normal resolution for other isotopes.

Data acquisition was performed in time-resolved mode. Dwell time for each isotope was 0.01 second. The gas background was measured for 20 seconds, while the dwell time of each laser spot was 40 seconds. To eliminate surface contamination, only the second half (20-second ablation time) of the laser profile was used in the calculations. Data was processed by Qtegra software. The LA-ICP-MS method was created to ensure the reproducibility of measurements and in order to be applicable for pearl identification submissions received by the laboratory. LA-ICP-MS is a quasi-nondestructive technique where the resulting tiny laser ablation spots are rarely visible without magnification. Further consideration is given to the position of analysis, which is usually carried out in an inconspicuous place that does not affect the visual appearance of the pearls (near the drill hole, the tapered end of a drop, or the flat base of a button). The round crater (laser spot) measures approximately 55 µm in diameter. The amount of nacre ablated from the two or three laser spots applied to each pearl is minimal and does not result in any noticeable weight loss.

LDA Methods. There are many statistical methods available that can model data in order to make predictions about unknown samples. Choosing the appropriate model depends on the type of data sought, whether or not information from *training classes*[1] is available, and the data's distribution (see box A). In this study, LDA was appropriate for origin determination of the three freshwater pearl types because the densities of the sample clusters with respect to various element concentrations have an approximately normal distribution. Cross-validation testing in-

---

[1] In this context, *training classes* are composed of samples sorted into specific categories that the statistical model is working to predict.

TABLE 2. Interferences of molecules and multiply charged ions on isotopes of interest.

Isotope	Atomic mass-ionic charge ratio of isotope	Interference in calcium carbonate (stalagmite)	Atomic mass-ionic charge ratio of interference	Interference in percentage of total counts	Required MRP to separate	MRP applied by LA-ICP-MS	Able to resolve from interference?
$^{7}\mathrm{Li}^{+}$	7.016004	$^{14}\mathrm{N}^{++}$	7.001537	>10%	485	10	No
$^{11}\mathrm{B}^{+}$	11.009305	$^{22}\mathrm{Ne}^{++}$	10.995693	1%–10%	809	16	No
$^{23}\mathrm{Na}^{+}$	22.989770	$^{46}\mathrm{Ca}^{++}$	22.976846	<1%	1779	33	No
$^{24}\mathrm{Mg}^{+}$	23.985042	$^{48}\mathrm{Ca}^{++}$	23.976267	>10%	2733	34	No
$^{31}\mathrm{P}^{+}$	30.973762	$^{15}\mathrm{N}^{16}\mathrm{O}^{+}$	30.995024	1%–10%	1457	44	No
		$^{14}\mathrm{N}^{17}\mathrm{O}^{+}$	31.002206	1%–10%	1089	44	No
$^{39}\mathrm{K}^{+}$	38.963707	$^{38}\mathrm{Ar}^{1}\mathrm{H}^{+}$	38.970557	1%–10%	5688	56	No
$^{43}\mathrm{Ca}^{+}$	42.958767	$^{86}\mathrm{Kr}^{++}$	42.955305	<1%	12409	143	No
$^{44}\mathrm{Ca}^{+}$	43.955481	$^{40}\mathrm{Ar}^{4}\mathrm{He}^{+}$	43.964986	<1%	4624	63	No
		$^{12}\mathrm{C}^{16}\mathrm{O}_2^{+}$	43.989830	<1%	1280	63	No
$^{47}\mathrm{Ti}^{+}$	46.951764	$^{15}\mathrm{N}^{16}\mathrm{O}_2^{+}$	46.989939	1%–10%	1230	67	No
		$^{14}\mathrm{N}^{16}\mathrm{O}_2{}^{1}\mathrm{H}^{+}$	47.000729	1%–10%	959	67	No
		$^{12}\mathrm{C}^{16}\mathrm{O}^{18}\mathrm{O}^{1}\mathrm{H}^{+}$	47.001900	1%–10%	936	67	No
$^{53}\mathrm{Cr}^{+}$	52.940654	$^{40}\mathrm{Ar}^{13}\mathrm{C}^{+}$	52.965738	>10%	2111	76	No
		$^{40}\mathrm{Ca}^{13}\mathrm{C}^{+}$	52.965946	>10%	2093	76	No
$^{55}\mathrm{Mn}^{+}$	54.938050	$^{40}\mathrm{Ar}^{15}\mathrm{N}^{+}$	54.962492	1%–10%	2248	78	No
$^{57}\mathrm{Fe}^{+}$	56.935399	$^{40}\mathrm{Ca}^{16}\mathrm{O}^{1}\mathrm{H}^{+}$	56.965331	>10%	1902	81	No
$^{59}\mathrm{Co}^{+}$	58.933200	$^{43}\mathrm{Ca}^{16}\mathrm{O}^{+}$	58.953682	>10%	2877	84	No
		$^{40}\mathrm{Ca}^{18}\mathrm{O}^{1}\mathrm{H}^{+}$	58.969576	>10%	1620	84	No
$^{60}\mathrm{Ni}^{+}$	59.930791	$^{44}\mathrm{Ca}^{16}\mathrm{O}^{+}$	59.950396	>10%	58	84	Yes
$^{63}\mathrm{Cu}^{+}$	62.929601	$^{27}\mathrm{Al}^{36}\mathrm{Ar}^{+}$	62.949084	1%–10%	3230	90	No
		$^{23}\mathrm{Na}^{40}\mathrm{Ar}^{+}$	62.952153	1%–10%	2790	90	No
$^{66}\mathrm{Zn}^{+}$	65.926037	Interference-free	–	–	–	–	–
$^{69}\mathrm{Ga}^{+}$	68.925581	$^{29}\mathrm{Si}^{40}\mathrm{Ar}^{+}$	68.938878	>10%	5184	98	No
		$^{138}\mathrm{Ba}^{++}$	68.952911	>10%	2522	98	No
$^{88}\mathrm{Sr}^{+}$	87.905614	$^{176}\mathrm{Yb}^{++}$	87.971284	<1%	1339	126	No
		$^{176}\mathrm{Lu}^{++}$	87.971341	<1%	1337	126	No
$^{89}\mathrm{Y}^{+}$	88.905848	Interference-free	–	–	–	–	–
$^{95}\mathrm{Mo}^{+}$	94.905841	Interference-free	–	–	–	–	–
$^{137}\mathrm{Ba}^{+}$	136.905821	Interference-free	–	–	–	–	–
$^{139}\mathrm{La}^{+}$	138.906348	Interference-free	–	–	–	–	–
$^{208}\mathrm{Pb}^{+}$	207.976636	Interference-free	–	–	–	–	–

Modified after Jochum et al. (2012).
Following the trial (test) work, these were considered the elements most likely to assist in separating the different types of freshwater pearls in this study. Rows highlighted in gray are the elements selected as "good discriminators."
$^{43}\mathrm{Ca}^{+}$ was measured under high-resolution mode. Everything else was measured under normal resolution mode. $^{60}\mathrm{Ni}^{+}$ was the only isotope LA-ICP-MS could resolve from interferences.

volved removing each sample from the aforementioned classes, training the LDA on the remaining samples, and then applying the LDA prediction on the removed sample. This robustness test yielded prediction rates only slightly lower than focusing the LDA with all available samples and then predicting to which class those same samples belong, indicating that the LDA method had sufficient training samples to maintain high prediction rates if additional pearls with the same origins were added. Pairwise analysis was applied, similar to the study by Luo et al. (2015), because otherwise the discriminant functions will change as more classes are added. Elements useful for the separation of two classes may not be useful for a third or fourth class. The authors introduced a decision tree to allow for the additional sophistication of classifying unknown samples as "undetermined" if there are contradictory results between pairwise tests or if unknown samples fall far from the clusters of known samples analyzed. However, no unknown samples were run in this experiment. In developing the LDA model, we collected multiple spots of chemical analysis for each pearl. Each spot was treated as a separate sample unit. The number of pearls and associated spots for each type of pearl are shown in table 1.

Pairwise LDA formulas were developed in which two functions are formulated: Each function computes a score for each pearl type. The higher score indicates a sample's pearl type. When running a pairwise LDA, a cross-validation method is applied to test the robustness of the model, whereby each pearl sample is classified by the functions derived from every other pearl sample. To make a final prediction, we constructed a simple *decision tree*[2] that merged the pairwise results into a single final result. If two out of three pairwise tests yielded the same result, then that "consensus" result became the final prediction. For example, if 1 vs. 2 = 2, and 1 vs. 3 = 1, and 2 vs. 3 = 2, then the predicted result would be "2." If no pearl types are selected twice, then the prediction becomes a fourth class: "undetermined." Note that in this study, an "undetermined" result was considered an incorrect prediction.

LA-ICP-MS AND LDA RESULTS

Chemical data recorded for the 22 elements selected are shown in table 3. The three types of freshwater pearls showed similar Ca concentrations. Of the trace elements analyzed, Na, Mn, Sr, and Ba were found to be useful discriminators based on careful examination of data with standard chemistry plots. ^{23}Na^{+} and ^{88}Sr^{+} had major interferences that were less than 1% of total counts, while ^{55}Mn^{+} had major interferences between 1% and 10% of total counts and ^{137}Ba^{+} had no major interference (see table 2, highlighted gray). Li, Na, Mg, Mn, Sr, and Ba have been proven to be useful discriminators when identifying marine aragonites (otolith) (Veinott and Porter, 2005; Sturgeon et al., 2005; Lara et al., 2008). However, Li and Mg both had interferences greater than 10% of the total counts (see table 2) and thus could not be corrected sufficiently by subtracting only the gas blank. Therefore, they were not used in the method because of the limitations of the instrument.

Seven of the USA-NAT samples contained Mn contents of less than 100 ppmw, which is unusual for freshwater pearls. Mn is generally above 100 ppmw in freshwater pearls and shells, but is low or even absent in saltwater material. The low Mn content of the seven samples suggests that they could be saltwater pearls. To verify the growth environment of these questionable samples, three extra spots were tested on each sample; the results are presented in table 4. All questionable samples contained low Sr (<1100 ppmw), low Na (<2100 ppmw), and high Ba (>30 ppmw), which is the opposite of the trace element results that were documented on known saltwater origin pearls from the *Pinctada maxima* mollusk (Scarratt et al., 2012; Sturman et al., 2016). A ternary diagram of Ba, Mg, and Mn (figure 2) was used to plot all studied freshwater and known saltwater pearls for better clarification. Moreover, additional groups of South Sea and Tahitian pearls that were analyzed by the same method used for the freshwater pearls were included in the diagram for supporting information. All the questionable samples plotted alongside the freshwater pearls, which showed that the samples likely have a freshwater rather than saltwater origin.

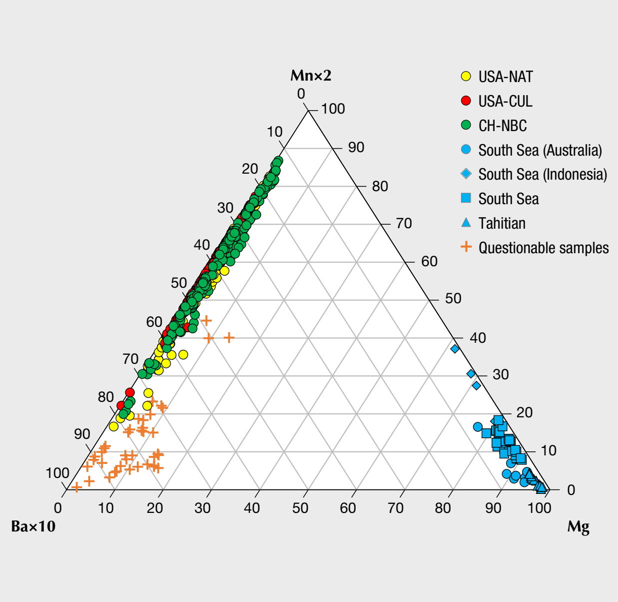

Figure 2. This ternary diagram of the relative percentages of Ba, Mg, and Mn shows clear separation between freshwater and saltwater pearls. All the questionable samples plotted alongside the freshwater pearls, indicating a likely freshwater rather than saltwater origin.

A chemical plotting method was used to plot the chemistry. The nine categories listed in table 5 represent different chemical ranges that were defined according to the concentrations of Sr and Ba. In order to reduce the overlapping areas among the three groups as much as possible, the boundaries of each

---

[2] A *decision tree* is a flowchart tool where each starting node is a test on an attribute, each branch is an outcome of the test, and each leaf (or final node) is a class.

TABLE 3. LA-ICP-MS chemical composition ranges of American and Chinese freshwater pearls studied (in ppmw).

	USA-NAT			USA-CUL			CH-NBC		
Elements	Maximum	Minimum	Average	Maximum	Minimum	Average	Maximum	Minimum	Average
Li	4.16	bdl	0.052	2.53	bdl	0.10	0.85	bdl	0.013
B	10.8	bdl	3.93	14.4	1.51	4.03	14.2	1.09	4.50
Na	2300	460	1710	2300	1050	1850	2870	879	2146
Mg	908	12.1	50.0	376	22.2	38.0	108	7.82	33.4
P	3260	bdl	251	693	bdl	230	315	bdl	207
K	162	bdl	9.49	518	bdl	8.04	64.6	bdl	10.7
Ca	422,000	384,000	407,000	427,000	359,000	407,000	441,000	324,000	403,000
Ti	bdl	bdl	bdl	58.8	bdl	0.48	1.23	bdl	0.018
Cr	24.7	bdl	0.13	5.38	bdl	0.048	2.24	bdl	0.026
Mn	2860	10.1	732	4080	667	1910	3330	185	856
Fe	973	126	319	1120	231	290	456	254	356
Co	0.50	bdl	0.13	0.43	bdl	0.11	0.81	0.082	0.16
Ni	134	bdl	1.15	184	bdl	1.39	1.94	0.40	0.71
Cu	8.52	bdl	0.71	9.77	bdl	0.32	0.73	bdl	0.25
Zn	3.92	bdl	0.55	8.24	bdl	0.86	4.32	bdl	0.88
Ga	22.6	1.20	5.03	45.5	3.29	13.0	17.4	0.44	5.67
Sr	1280	150	382	707	346	505	986	238	470
Y	0.13	bdl	0.004	0.52	bdl	0.009	0.12	bdl	0.004
Mo	0.14	bdl	0.010	0.18	bdl	0.023	0.17	bdl	0.013
Ba	441	23.8	111	1360	82.6	300	324	11.1	112
La	0.25	bdl	0.006	0.93	bdl	0.010	0.29	bdl	0.009
Pb	0.21	bdl	0.017	1.27	bdl	0.017	0.83	bdl	0.027

Detection limits: Li (0.027–0.26), B (0.23–0.63), Na (0.73–40.5), Mg (0.015–0.096), P (2.83–27.2), K (1.40–1.02), Ca (15.7–75.4), Ti (0.13–0.36), Cr (0.16–0.59), Mn (0.10–1.04), Fe (1.26–3.37), Co (0.009–0.023), Ni (0.026–6.36), Cu (0.024–0.43), Zn (0.097–0.56), Ga (0.013–0.84), Sr (0.014–0.14), Y (0.001–0.003), Mo (0.004–0.027), Ba (0.005–0.14), La (0.001–0.031), Pb (0.004–0.16).
bdl: below detection limit.
If the value is larger than or equal to 1, we use three significant figures. For example, 3260, 908, 24.7, and 1.15.
If the value is smaller than 1 and larger than or equal to 0.01, we use two significant figures. For example, 0.50 and 0.023.
If the value is smaller than 0.01, we use one significant figure. For example, 0.006.
All data in this article is presented by following the significant figure rule.

category were determined based on the analytical data and authors' experience. This method is modified based on geographic origin plots for sapphires used internally by GIA (A. Palke, pers. comm., 2018). Mn-Na corresponding chemical plots were constructed for each Ba-Sr category (figure 3). These categories showed it was easy to separate the USA-CUL pearls from the USA-NAT and CH-NBC pearls. In the low Ba, low Sr category (figure 3A), all USA-CUL pearls were off the plot, which left only two groups (USA-NAT and CH-NBC). In the high Ba, high Sr category (figure 3B), the majority of USA-CUL pearls were in the plot, while a high proportion of pearls from the other two groups were off the plot. Aside from these results, partial separation may also be made using the high Ba, medium Sr (figure 3H) and medium Ba, medium Sr (figure 3I) categories.

The Mn concentrations were high in all the USA-CUL samples, with none less than 650 ppmw. The USA-CUL samples all had Sr or Ba contents greater than 340 and 80 ppmw, respectively. These samples are easier to identify through the narrower range in trace elements, because they were farmed from a single location and mollusk species. The USA-NAT and CH-NBC both showed many overlapping trace elements, most likely because the natural pearls formed in many mussel species spread across a large geographic footprint in North America. In the case

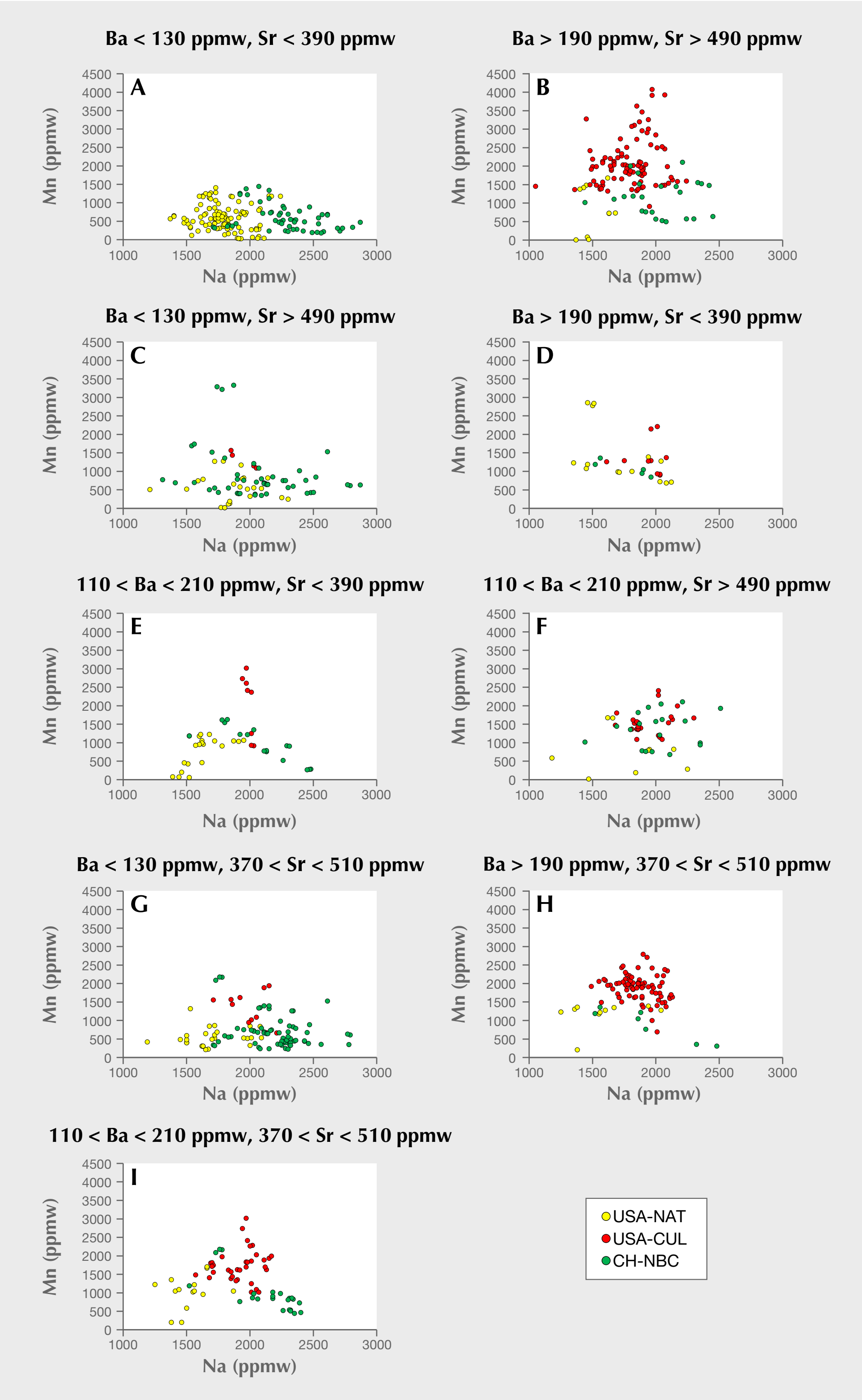

Figure 3. Mn vs. Na plots for the three freshwater pearl groups in each Ba-Sr category, modified from selective chemistry plots for the geographic origin of corundum.

of the Chinese pearls, the samples were obtained from different pearl dealers who no doubt acquired them from different culturing areas, also distributed over a wide geographic area. Nonetheless, they did reveal a degree of separation when specific parameters were applied. Of the samples studied, only the

TABLE 4. LA-ICP-MS trace-element results (in ppmw) on questionable pearl samples.

Sample	Li	B	Na	Mg	P	K	Mn	Fe	Zn	Sr	Ba
NAT-EB2 SP1	bdl	2.36	2070	47.7	362	8.28	90.3	262	2.40	172	54.7
NAT-EB2 SP2	bdl	2.90	2020	47.9	368	7.81	64.3	265	2.22	170	47.1
NAT-EB2 SP3	bdl	0.91	1980	32.2	240	8.70	54.1	329	1.33	144	43.9
NAT-EB2 SP4	bdl	0.72	1960	31.8	253	7.55	48.9	330	1.31	151	48.6
NAT-EB2 SP5	bdl	0.79	1930	33.6	257	6.19	49.2	327	1.36	153	51.7
NAT-USA5 SP1	bdl	2.62	2060	133	243	15.6	42.1	291	0.93	332	70.2
NAT-USA5 SP2	bdl	2.65	1900	134	252	14.3	44.5	298	0.98	342	72.2
NAT-USA5 SP3	bdl	2.36	2110	135	263	13.9	42.2	296	0.99	355	75.7
NAT-USA5 SP4	bdl	0.54	1850	96.4	192	19.8	24.7	328	0.61	333	78.1
NAT-USA5 SP5	bdl	bdl	1780	103	190	11.3	26.6	330	0.66	319	72.3
NAT-USA5 SP6	bdl	bdl	1800	112	192	10.9	28.0	328	0.56	300	66.8
NAT-USA12 SP1	bdl	4.19	1460	89.2	165	117	83.3	279	0.42	546	210
NAT-USA12 SP2	bdl	4.07	1470	73.0	116	162	22.7	290	0.84	511	192
NAT-USA12 SP3	bdl	4.47	1370	56.0	99.2	21.4	10.1	288	0.47	780	303
NAT-USA12 SP4	bdl	bdl	1900	77.5	225	7.03	260	331	0.26	277	56.9
NAT-USA12 SP5	bdl	bdl	1930	176	230	bdl	260	327	0.51	274	60.1
NAT-USA12 SP6	bdl	bdl	1910	105	230	bdl	223	332	bdl	272	56.5
NAT-USA21 SP1	bdl	3.35	1920	28.1	229	7.02	28.4	349	1.28	212	27.9
NAT-USA21 SP2	bdl	3.22	1930	27.6	225	5.10	29.6	359	1.35	204	27.6
NAT-USA21 SP3	bdl	3.58	1910	24.1	216	4.04	32.9	347	1.40	201	26.9
NAT-USA21 SP4	bdl	0.54	1910	29.6	270	9.36	11.4	334	3.32	230	31.4
NAT-USA21 SP5	bdl	0.42	1910	32.3	266	7.72	15.5	302	2.93	230	32.2
NAT-USA21 SP6	bdl	0.53	1940	30.4	262	8.20	18.0	329	2.92	237	33.2
NAT-USA26 SP1	bdl	4.97	1770	70.0	253	18.9	21.4	385	0.99	896	77.1
NAT-USA26 SP2	bdl	5.37	1800	67.9	262	19.8	15.3	378	0.95	944	84.0
NAT-USA26 SP3	bdl	4.87	1800	66.4	259	16.0	19.8	377	1.28	905	75.6
NAT-USA26 SP4	bdl	1.73	2030	83.0	207	7.65	17.8	327	1.70	632	43.7
NAT-USA26 SP5	bdl	1.47	1990	84.5	207	6.64	17.2	329	1.64	623	44.3
NAT-USA26 SP6	bdl	1.54	2000	93.9	204	5.68	16.6	327	1.64	621	45.5
NAT-ANP14 SP1	bdl	8.11	1440	30.7	bdl	bdl	73.3	269	bdl	346	168
NAT-ANP14 SP2	bdl	5.92	1390	27.9	bdl	bdl	81.9	259	bdl	348	168
NAT-ANP14 SP3	bdl	7.09	1520	25.9	bdl	bdl	62.8	264	bdl	341	190
NAT-ANP14 SP4	bdl	bdl	1620	31.8	273	14.5	68.6	313	0.24	346	121
NAT-ANP14 SP5	bdl	bdl	1630	30.3	274	13.5	71.1	309	0.25	337	113
NAT-ANP14 SP6	bdl	bdl	1590	28.0	273	12.8	70.8	309	0.26	328	106
NAT-HS2 SP1	bdl	2.81	1840	97.7	313	26.7	127	261	1.71	1000	79.4
NAT-HS2 SP2	bdl	2.53	1830	99.7	311	27.5	118	256	0.93	1020	75.8
NAT-HS2 SP3	bdl	bdl	1810	82.6	227	29.9	76.7	327	0.59	964	76.5
NAT-HS2 SP4	bdl	bdl	1850	97.4	234	18.3	70.9	329	0.36	1000	70.1
NAT-HS2 SP5	bdl	0.47	1780	104	254	21.2	51.8	327	0.26	1020	93.7

bdl = below detection limit

USA-NAT samples (14%) had both Na contents of less than 2000 ppmw and Mn contents of less than 320 ppmw. USA-NAT samples showed Sr concentrations below 230 ppmw (9%) and Mn concentrations below 180 ppmw (10%). Only CH-NBC samples (31%) had Na concentrations over 2300 ppmw. None of the other sample groups showed these concentrations.

In general, the American samples showed Na levels lower than 2000 ppmw (USA-NAT 85% and USA-CUL 73%), while 69% of Chinese samples were higher than this amount. For the USA-CUL

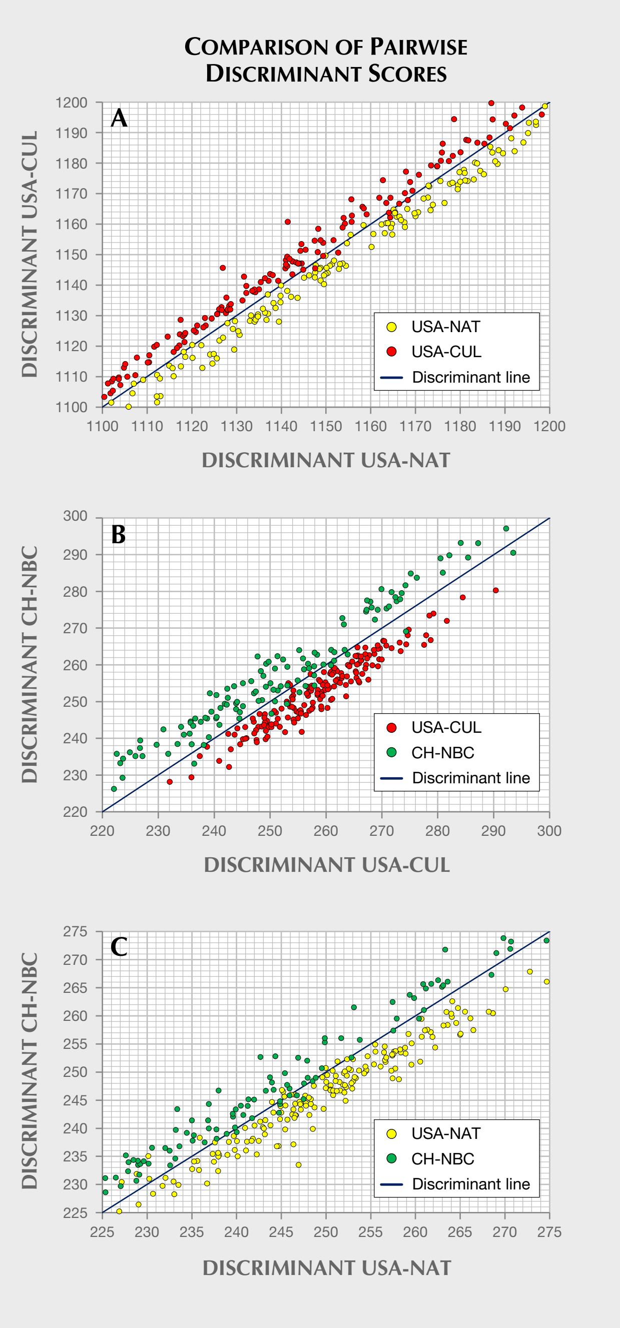

Figure 4. These three plots compare pairwise discriminant scores between American natural and American cultured samples (4A), Chinese NBC and American cultured samples (4B), and Chinese NBC and American natural samples (4C). For a pairwise LDA analysis, two discriminant functions are produced using a combination of the following elements: ^{23}Na, ^{39}K, ^{44}Ca, ^{55}Mn, ^{57}Fe, and ^{88}Sr. Applying the chemical concentrations for each sample into each of the two functions produces two scores, one representing each group. For each sample in the pairwise plots, the x-axis represents the score for one group and the y-axis represents the score for the other. In general, the relatively higher score indicates to which group the sample belongs. For example, samples from the CH-NBC group in figure 4B have a higher CH-NBC score in the y-axis direction relative to its USA-CUL score in the x-axis direction. The blue line separates the prediction of the two groups. The area above the blue line predicts that the sample belongs to the group on the y-axis; below the blue line predicts that the sample belongs to the group on the x-axis.

samples, 73% showed high Mn (>1000 ppmw) and Ba (>200 ppmw). Conversely, 82% of USA-NAT and 75% of CH-NBC samples showed low Mn (<1500 ppmw) and Ba (<200 ppmw). Sr concentration was high (>400 ppmw) in 88% of the USA-CUL samples, low (<400 ppmw) in 68% of the USA-NAT samples, and medium (300 to 600 ppmw) in 77% of the CH-NBC samples. All the percentages reported are based on the numbers of samples studied, rather than the number of analyzed spots.

The chemical characteristics of the freshwater pearl samples enabled a relatively well-defined separation to be carried out using the LDA application we developed. A combination of the following elements was found to be most useful for the separation of the different groups: ^{23}Na, ^{39}K, ^{44}Ca, ^{55}Mn, ^{57}Fe, and ^{88}Sr. For a pairwise LDA model, two discriminant functions were constructed and predicted two scores, one for each group. In general, the higher score indicated to which group the sample belonged. A model that predicts 100% places all samples correctly into the known groups. For the pair USA-NAT vs. USA-CUL, the (non-cross-validated) discriminant scores are plotted in figure 4A with the overall trend for USA-NAT samples to have higher USA-NAT discriminant scores relative to USA-CUL scores and with USA-CUL samples showing the opposite trend. Although the separation between the two groups looks small, 92.6% of the cross-validated grouped cases were correctly predicted. Thus, the model is a very good predictor, with the cross-validation test confirming the model's statistical validity. For the USA-CUL vs. CH-NBC and USA-NAT vs. CH-NBC pairs, the cross-validated prediction rates were 87.7% and 87.6%, respectively (figures 4B and 4C). The percentage of all the samples correctly predicted by the final decision tree step into the three known groups was over 85%. There are a number of factors such as varying species, location, and environment that could be contributing

TABLE 5. Sample categories defined by Ba and Sr concentration ranges (in ppmw[a]).

Category	Ba range	Sr range	Corresponding plot
Low Ba, Low Sr	Ba<130	Sr<390	Figure 3A
High Ba, High Sr	Ba>190	Sr>490	Figure 3B
Low Ba, High Sr	Ba<130	Sr>490	Figure 3C
High Ba, Low Sr	Ba>190	Sr<390	Figure 3D
Medium Ba, Low Sr	110<Ba<210	Sr<390	Figure 3E
Medium Ba, High Sr	110<Ba<210	Sr>490	Figure 3F
Low Ba, Medium Sr	Ba<130	370<Sr<510	Figure 3G
High Ba, Medium Sr	Ba>190	370<Sr<510	Figure 3H
Medium Ba, Medium Sr	110<Ba<210	370<Sr<510	Figure 3I

[a]A 20 ppmw overlapping area was defined between each adjacent category to account for analytical error.
Pearls showing chemistry within the overlapping areas were included in plots in figure 3.

to the variance in sample chemistry, making the task of predicting these groups correctly more difficult. Despite such potential sources of variance, the LDA empirically predicts much better than chance. So at least for the samples tested, there are tendencies in chemistry that can be applied broadly to China, for example, that do not apply to the United States. Nevertheless, collections of samples that better represent any important factors contributing to the variance can lead to models that accommodate the influence of those additional factors, thereby improving upon the current prediction rates.

Lastly, the chemical plots comparing Sr and Na contents (figure 5) revealed a large number of USA-NAT and CH-NBC samples that exhibited challenging internal growth structures and were difficult to identify with X-ray techniques, thus separating them from the other sample groups. All the measurement spots of the studied samples are displayed in the plot, and concentrations of Sr and Na of these specific samples are shown in table 6. The LDA method correctly discriminated 60% and 70% of these challenging USA-NAT and CH-NBC samples, respectively (again, see table 6, column 4).

CONCLUSIONS

From the findings of this preliminary study, we propose that the combination of trace-element information provided by LA-ICP-MS and subsequent application of LDA has the potential to classify freshwater pearls from different sources with relatively reliable accuracy. This method can be a useful aid in identifying freshwater pearls exhibiting challenging internal growth structures. The samples studied here were not collected directly from the mollusks (but

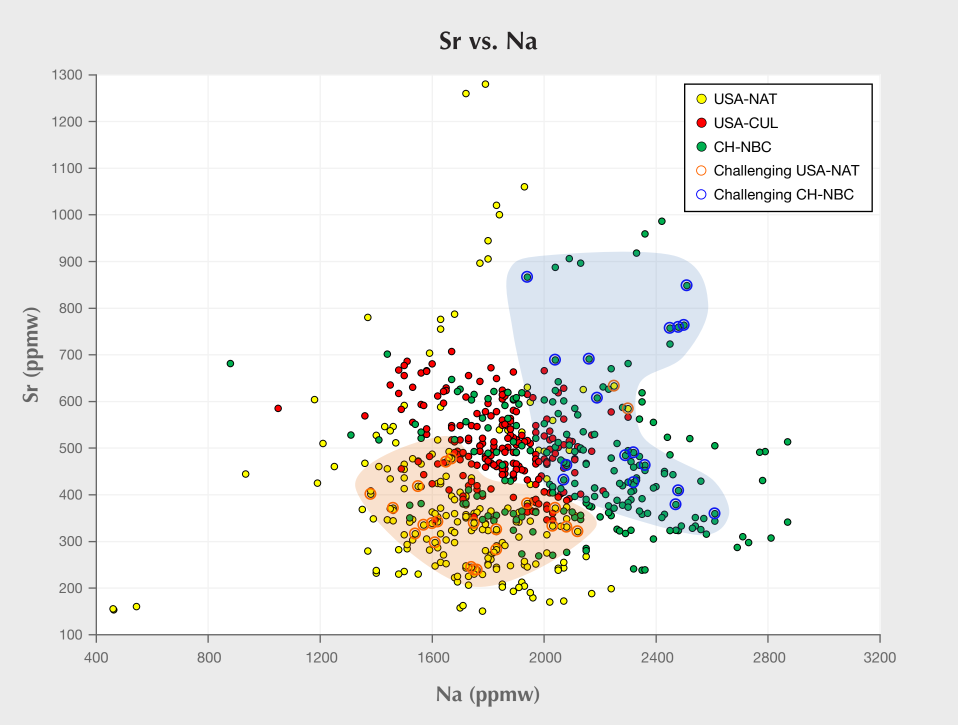

Figure 5. The chemical plot of Sr vs. Na contents shows that a large number of American natural (orange shaded area) and Chinese NBC (blue shaded area) samples exhibited challenging internal growth structures and were difficult to identify using X-ray techniques, thus separating them from the other sample groups.

TABLE 6. Na and Sr concentrations (in ppmw) of challenging American natural and Chinese NBC samples.

USA-NAT				CH-NBC			
Sample	Na[a]	Sr[a]	LDA[b]	Sample	Na[a]	Sr[a]	LDA[b]
NAT-TR1 SP1	1670	477	USA-NAT	NBC-CH5 SP1	2510	848	CH-NBC
NAT-TR1 SP2	1650	470	USA-NAT	NBC-CH5 SP2	1940	866	CH-NBC
NAT-TR3 SP1	2080	331	USA-CUL	NBC-CH9 SP1	2070	432	CH-NBC
NAT-TR3 SP2	2030	333	USA-CUL	NBC-CH9 SP2	2080	463	CH-NBC
NAT-TR3 SP3	2120	321	USA-CUL	NBC-CH12 SP1	2610	359	CH-NBC
NAT-TR4 SP1	1750	239	USA-NAT	NBC-CH12 SP2	2470	379	CH-NBC
NAT-TR4 SP2	1760	239	USA-NAT	NBC-CH15 SP1	2480	409	USA-CUL
NAT-TR4 SP3	1740	244	USA-NAT	NBC-CH15 SP2	2320	426	USA-CUL
NAT-MIX1 SP1	1550	418	USA-NAT	NBC-CH16 SP1	2480	759	CH-NBC
NAT-MIX1 SP2	1610	297	USA-NAT	NBC-CH16 SP2	2500	763	CH-NBC
NAT-USA1 SP1	2040	371	USA-CUL	NBC-CH16 SP3	2450	757	CH-NBC
NAT-USA1 SP2	1940	381	USA-CUL	NBC-CH35 SP1	2290	484	CH-NBC
NAT-USA2 SP1	2250	633	CH-NBC	NBC-CH35 SP2	2320	490	CH-NBC
NAT-USA2 SP2	2300	584	CH-NBC	NBC-CH35 SP3	2360	463	CH-NBC
NAT-USA17 SP1	1620	342	USA-NAT	NBC-CHRB3 SP1	2190	607	CH-NBC
NAT-USA17 SP2	1600	338	USA-NAT	NBC-CHRB3 SP2	2160	691	USA-CUL
NAT-USA17 SP3	1570	335	USA-NAT	NBC-CHRB3 SP3	2040	689	USA-CUL
NAT-USA18 SP1	1460	371	USA-NAT				
NAT-USA18 SP2	1380	401	USA-NAT				
NAT-USA18 SP3	1540	316	USA-NAT				
NAT-ANP04 SP1	1750	339	USA-NAT				
NAT-ANP04 SP2	1830	325	USA-NAT				
NAT-ANP04 SP3	1830	282	USA-NAT				

[a] *Plotted in figure 5.*
[b] *LDA-predicted results. Gray shading indicates challenging samples that were not correctly discriminated.*

were supplied by reliable sources), and we cannot pinpoint the exact locations within the sources. The trace-element variations nonetheless corresponded to the geographic location, water environment, and mollusk species in which the pearls formed, and the results confirmed a degree of variation among sources.

To improve the usefulness of this technique to laboratory gemologists, we intend to study additional known samples from various geographic locations so that a large and dependable data set can be developed. The data may be further enhanced by narrowing down the recorded sources, as the results on the group of USA-CUL samples included in this work proves, by collecting pearls directly from specific localities, harvest seasons, and mollusk species, whether they be natural pearls from Tennessee and Colorado in the United States, Scotland, or Germany, or NBC pearls from China, Japan, Thailand, or Vietnam, among other possibilities.

Pearl identification is still carried out primarily by observing and interpreting the structural results obtained from various X-ray techniques, and our method can only be used to support those results. Yet in cases where all the structural evidence has been destroyed by the drilling process or where the structure is so subjective that different opinions exist within the same laboratory, let alone between different laboratories, the combination of LA-ICP-MS and LDA may be the only way to reach a conclusion other than undeterminable. The only other possible aid to identification in the most challenging of cases is DNA testing, and this is another area of ongoing research for GIA and other institutes.

ABOUT THE AUTHORS

Ms. Homkrajae is a senior staff gemologist in pearl identification, Mr. Sun is a research associate, and Dr. Blodgett is a research scientist at GIA in Carlsbad, California. Dr. Zhou is a research scientist and the manager of pearl identification at GIA in New York.

ACKNOWLEDGMENTS

The authors wish to thank Gina Latendresse of the American Pearl Company, Inc. for providing the American pearl samples and information on them. Dr. Aaron Palke at GIA Carlsbad is kindly thanked for his guidance in helping us establish and standardize the method of making selective pearl chemical plots in different chemical ranges. We are deeply grateful to Dr. Zhongxing Chen at Harvard University's Department of Earth and Planetary Sciences for providing valuable advice to optimize LA-ICP-MS instrumental conditions, and sharing expertise in analyzing marine aragonites. Assistance from Daniel Girma at GIA's New York laboratory in finalizing the analytical procedure is greatly appreciated. Joyce WingYan Ho and Sally Chan Shih, also of GIA in New York, are thanked for their assistance with the examination of the internal structures and carrying out X-ray fluorescence analysis on the samples. Lastly, we thank Nicholas Sturman at GIA Bangkok for his helpful and constructive feedback.

REFERENCES

Abduriyim A., Kitawaki H. (2006) Applications of laser ablation-inductively coupled plasma-mass spectrometry (LA-ICP-MS) to gemology. *G&G*, Vol. 42, No. 2, pp. 98–118, http://dx.doi.org/10.5741/GEMS.42.2.98

Akamatsu S., Li T.Z., Moses T.M., Scarratt K. (2001) The current status of Chinese freshwater cultured pearls. *G&G*, Vol. 37, No. 2, pp. 96–113, http://dx.doi.org/10.5741/GEMS.37.2.96

Blodgett T.A., Shen A.H. (2011) Application of discriminant analysis in gemology: Country-of-origin separation in colored stones and distinguishing HPHT-treated diamonds. *G&G*, Vol. 47, No. 2, p. 145.

China Gems (2019) Current status and development of the pearl industry, https://mp.weixin.qq.com/s/IdSPt0KRmhvPKg4kKeB RrQ [in Chinese].

Dumańska-Słowik M., Heflik W., Natkaniec-Nowak L., Sikorska M., Wesełucha-Birczyńska A. (2008) Cultured freshwater pearls from the Yangtze River (China); characterisation by optical microscopy, scanning electron microscopy, cathodoluminescence, electron microprobe analysis, and Raman spectroscopy. *The Australian Gemmologist*, Vol. 23, No. 7, pp. 290–299.

Fiske D., Shepherd J. (2007) Continuity and change in Chinese freshwater pearl culture. *G&G*, Vol. 43, No. 2, pp. 138–145, http://dx.doi.org/10.5741/GEMS.43.2.138

Friedman J.H. (1989) Regularized discriminant analysis. *Journal of the American Statistical Associatio*n. Vol. 84, No. 405, pp. 165–175.

Giuliani G., Caumon G., Rakotosamizany S., Ohnenstetter D., Rakotondrazafy M. (2014) Classification chimique des corindons par analyse factorielle discriminante: application a la typologie des gisements de rubis et saphirs. *Revue de l'Association Francaise de Gemmologie*, No. 188, pp. 14–22.

Grabarkiewicz J.D., Davis W.S. (2008) An Introduction to Freshwater Mussels as Biological Indicators: Including Accounts of Interior Basin, Cumberlandian, and Atlantic Slope Species. United States Environmental Protection Agency, Washington, DC, http://dx.doi.org/10.13140/2.1.3580.2405

Haag W.R. (2012) *North American Freshwater Mussels: Natural History, Ecology, and Conservation*. Cambridge University Press, Cambridge, UK.

Habermann D., Banerjee A., Meijer J., Stephan A. (2001) Investigation of manganese in salt-and freshwater pearls. *Nuclear Instruments and Methods in Physics Research Section B: Beam Interactions with Materials and Atoms*, Vol. 181, No. 1-4, pp. 739–743, http://dx.doi.org/10.1016/S0168-583X(01)00353-6

Hänni H.A., Kiefert L., Giese P. (2005) X-ray luminescence, a valuable test in pearl identification. *The Journal of Gemmology*, Vol. 29, No. 5/6, pp. 325–329.

Hastie T., Tibshirani R., Friedman J. (2009) *The Elements of Statistical Learning: Data Mining, Inference, and Prediction*, 2nd ed. Springer-Verlag, New York, 745 pp., https://www.springer.com/us/book/9780387848570

Hsu T., Zhou C., Homkrajae A., Ho J.W.Y., Yazawa E., Padua P. (2016) Freshwater pearling in Tennessee. *GIA Field Report*, https://www.gia.edu/gia-news-research/freshwater-pearling-tennessee

Hsu T., Zhou C., Homkrajae A., Ho J.W.Y., Yazawa E., Padua P. (2017) The lure of American freshwater pearls: Revisiting the Latendresse family. *GIA Field Report*, https://www.gia.edu/gia-news-research/lure-american-freshwater-pearls-revisiting-latendresse-family

Hua D., Gu R. (2002) Freshwater pearl culture and production in China. *Aquaculture Asia*, Vol. 7, No. 1, pp. 6–8.

Jochum K.P., Scholz D., Stoll B., Weis U., Wilson S.A., Yang Q., Schwalb A., Börner N., Jacob D.E., Andreae M.O. (2012) Accurate trace element analysis of speleothems and biogenic calcium carbonates by LA-ICP-MS. *Chemical Geology*, Vol. 318, pp. 31–44, http://dx.doi.org/10.1016/j.chemgeo.2012.05.009

Karampelas S., Michel J., Zheng-Cui M., Schwarz J.-O., Enzmann F., Fritsch E., Leu L., Krzemnicki M.S. (2010) X-ray computed microtomography applied to pearls: Methodology, advantages, and limitations. *G&G*, Vol. 46, No. 2, pp. 122–127, http://dx.doi.org/10.5741/GEMS.46.2.122

Karampelas S., Al-Alawi A.T., Al-Attawi A. (2017) Real-time microradiography of pearls: A comparison between detectors. *G&G*, Vol. 53, No. 4, pp. 452–456, http://dx.doi.org/10.5741/GEMS.53.4.452

Kessrapong P., Lawanwong K., Sturman N. (2017) *Pinctada maculata* (pipi) bead-cultured blister pearls attached to their shells. *GIA Research News*, April 25, https://www.gia.edu/gia-news-research/pinctada-maculata-bead-cultured-blister-pearls-shells

Krzemnicki M., Friess D., Chalus P., Hänni H.A., Karampelas S. (2010) X-ray computed microtomography: Distinguishing natural pearls from beaded and non-beaded cultured pearls. *G&G*, Vol. 46, No. 2, pp. 128–134, http://dx.doi.org/10.5741/GEMS.46.2.128

Kunz G.F., Stevenson C.H. (1908) *The Book of the Pearl*. The Century Co., New York, pp. 485–513.

Lara M.R., Jones D.L., Chen Z., Lamkin J.T., Jones C.M. (2008) Spatial variation of otolith elemental signatures among juvenile gray snapper (*Lutjanus griseus*) inhabiting southern Florida waters. *Marine Biology*, Vol. 153, No. 3, pp. 235–248, http://dx.doi.org/10.1007/s00227-007-0799-5

Luo Z., Yang M., Shen A.H. (2015) Origin determination of dolomite-related white nephrite through iterative-binary linear discriminant analysis. *G&G*, Vol. 51, No. 3, pp. 300–311, http://dx.doi.org/10.5741/GEMS.51.3.300

Martinez A.M., Kak A.C. (2001) PCA versus LDA. *IEEE Transactions on Pattern Analysis and Machine Intelligence*, Vol. 23, No. 2, pp. 228–233, https://ieeexplore.ieee.org/document/908974

Pornwilard M.-M., Hansawek R., Shiowatana J., Siripinyanond A. (2011) Geographical origin classification of gem corundum using elemental fingerprint analysis by laser ablation-inductively coupled plasma-mass spectrometry. *International Journal of Mass Spectrometry*, Vol. 306, No. 1, pp. 57–62, http://dx.doi.org/10.1016/j.ijms.2011.06.010

Scarratt K., Moses T.M., Akamatsu S. (2000) Characteristics of nuclei in Chinese freshwater cultured pearls. *G&G*, Vol. 36, No. 2, pp. 98–109, http://dx.doi.org/10.5741/GEMS.36.2.98

Scarratt K., Bracher P., Bracher M., Attawi A., Safar A., Saeseaw S., Homkrajae A., Sturman N. (2012) Natural pearls from Australian *Pinctada maxima*. *G&G*, Vol. 48, No. 4, pp. 236–261, http://dx.doi.org/10.5741/GEMS.48.4.236

Shen A., Blodgett T., Shigley J. (2013) Country-of-origin determination of modern gem peridots from LA-ICPMS trace-element chemistry and linear discriminant analysis (LDA). *Geological Society of America Abstracts with Programs*, Vol. 45, No. 7, p. 525.

Strack E. (2006) *Pearls*. Rühle-Diebener-Verlag, Stuttgart, Germany, pp. 232–251.

Sturgeon R.E., Willie S.N., Yang L., Greenberg R., Spatz R.O., Chen Z., Sciver C., Clancy V., Lam J. W., Thorrold S. (2005) Certification of a fish otolith reference material in support of quality assurance for trace element analysis. *Journal of Analytical Atomic Spectrometry*, Vol. 20, No. 10, pp. 1067–1071, http://dx.doi.org/10.1039/b503655k

Sturman N. (2009) The microradiographic structures on non-bead cultured pearls. GIA Thailand, Bangkok, November 21, www.giathai.net/pdf/The_Microradiographic_structures_in_NBCP.pdf

Sturman N., Bergman J., Poli J., Homkrajae A., Manustrong A., Somsa-ard N. (2016) Bead-cultured and non-bead cultured pearls from Lombok, Indonesia. *G&G*, Vol. 52, No. 3, pp. 288–297, http://dx.doi.org/10.5741/GEMS.52.3.288

Sweaney J.L., Latendresse J.R. (1984) Freshwater pearls of North America. *G&G*, Vol. 20, No. 3, pp. 125–140, http://dx.doi.org/10.5741/GEMS.20.3.125

U.S. Fish & Wildlife Service (2018) Endangered species: America's mussels: Silent sentinels, https://www.fws.gov/midwest/endangered/clams/mussels.html

Veinott G., Porter R. (2005) Using otolith microchemistry to distinguish Atlantic salmon (*Salmo salar*) parr from different natal streams. *Fisheries Research*, Vol. 71, No. 3, pp. 349–355, http://dx.doi.org/10.1016/j.fishres.2004.09.004

Watters G.T., Hoggarth M.A., Stansbery D.H. (2009) *The Freshwater Mussels of Ohio*. The Ohio State University Press, Columbus.